

F023

## Efficient and Effective 3D Wavefield Tomography

M. Warner\* (Imperial College London), I. Stekl (Imperial College London) & A. Umpleby (Imperial College London)

### SUMMARY

---

We demonstrate 3D wavefield tomography applied to surface-streamer seismic data and obtain a result which appears to remove the distorting effects of shallow high-velocity channels. The methodology is of wide general applicability.

Full waveform seismic inversion, or wavefield tomography as it is also known, have become well established in two dimensions following the pioneering work of Gerhard Pratt and co-workers who developed the first frequency-domain direct solvers for the acoustic wave equation for cross-hole data. Their work has been extended and developed, and time-domain, visco-acoustic, elastic and anisotropic schemes have appeared in 2D, and these applied to a variety of source-receiver geometries. In the last year or two, these methods have begun to be extended into three-dimensions where their full potential can be realised. In this paper, we present one of the first studies to apply 3D wavefield tomography to field data, and demonstrate that the method can solve useful exploration problems that are not tractable by other methods.

In 2D, two principal methods have been used to perform wavefield tomography – direct factorisation of the matrix equations obtained by applying finite differences to the wave equation in the frequency domain, and explicit time-stepping of the finite difference equations in the time-domain. The two approaches both have their own advantages and problems, and both have recently been extended into three dimensions and applied to synthetic datasets. Both methods are computationally daunting in 3D.

We have chosen a third route; we solve the frequency-domain finite-difference matrix equations in 3D using an iterative rather than a direct solver. In this approach, we first solve an approximate matrix equation (the preconditioning matrix) for a particular source. This approximate solution is then substituted into the true matrix equations to derive a residual error. This error is then treated as a new source for which we can obtain an approximate solution, and the method is iterated. The advantage of this approach over that of a direct solution by, for example LU decomposition and nested dissection, is that the memory required in 3D is typically reduced by several orders of magnitude. Thus the iterative method can be implemented on a single workstation rather than distributed across a large cluster. The advantage over the time-domain method is that, provided that only a few frequencies are required for tomography, the compute time taken for one source is typically much less in the frequency domain than in the time domain.

There are also disadvantages of our method. Using a direct solution in the frequency domain has the advantage that multiple sources may be obtained relatively cheaply by back substitution once the initial factorisation has been completed. However, in 3D, the computational effort required to obtain an iterative solution for a single source is typically no larger than that required to obtain the solution by back substitution, but the memory required is much less. In the time-domain, there is a near-one-to-one relationship between a particular part of the seismic data and a particular part of the earth model. This means that simple processing of the seismic data, especially muting, weighting and filtering, can be readily integrated within a time-domain tomographic scheme, and readily quality controlled, in ways that are difficult or impossible in the sparse frequency-domain.

The key to obtaining an efficient and effective iterative solver is the appropriate choice of both the preconditioning matrix and the method used to calculate the iterative update. We have tried many variants of preconditioner and found that most methods that work well in other areas of computational physics perform badly or fail entirely for the wave equation. Currently we use three levels of preconditioner. At the lowest level, we use a simple one-way propagator that propagates energy a distance of about 20 cells across the model. We sweep this in six orthogonal

directions, up-down, back-front and left-right. This approximate solution is then iterated with the full two-way wave equation so that we obtain the full solution to the two-way equation.

At a higher level, we use a multi-grid approach. Here, we first solve the wave equation on a coarse grid. This coarse solution serves as a preconditioner for a more accurate solution on a finer grid. For the lowest frequencies, the coarsening of the mesh may involve several stages, halving the grid spacing at each step. We use a 27-point cubic finite-difference stencil that is formally second-order in space but which performs with a numerical accuracy equivalent to a conventional fourth-order stencil at a grid spacing of about 5 grid points per seismic wavelength. At the highest level, we divide the model into a small number of overlapping sub-domains. We solve first for the sub-domains separately, then use these as preconditioners to obtain the solution over the entire domain. The iterative updates use a restarted flexible generalise minimum residual (fGMRES) method, but we find that it is necessary only to store and use one generation of previous results to obtain optimal convergence which also minimise memory usage.

We have implemented this multi-preconditioned iterative forward solver within a parallel tomographic solver that is also iterative. Within the tomography there are two levels of parallelisation. A single (composite – see below) source is solved on a single multi-core/multi-CPU node. POSIX threads are used to balance the computation across all the cores present on the node. The node need be concerned only with that part of the physical model which its source illuminates and which produces seismic returns at its receivers. Typically this region is smaller than that of the global model.

Additional sources are computed in parallel on additional nodes, and a master node combines the individual results to provide a global update to the model, and control and balance the computation across the cluster. In an ideal case, the number of nodes will equal the number of sources plus the master node, and individual nodes will have the maximum number of economically available cores – currently eight as quad-core dual-CPU's. Where there are more sources than available nodes, multiple sources may be solved on a single node at a maximum of one source per core provided that there is sufficient memory. Where there is neither sufficient memory or sufficient cores, then multiple sources are solved sequentially on the same nodes.

A further enhancement is that we combine the data from individual point sources to form a smaller number of composite sources, and perform the tomography on these composite sources. Provided that the number of point sources mixed in this way is not too large, we find that there is no change in the quality of the velocity image that we obtain. The maximum number of sources that can be mixed in this way, and their optimum geometry depends upon the acquisition geometry and the details of the velocity model; this is still an area of active research. The optimum mix of point sources ranges from all of them combined to form a single composite source which is appropriate when the geometry of the tomographic coverage is near-complete, to around ten to twenty sources mixed together which is appropriate for conventional surface-streamer 3D swath shooting.

We have applied our tomographic scheme to the data shown in figure 1. These 3D data are from an 8-streamer dual-source flip-flop conventional swath survey in the North Sea with a cable length of 5000 m and cable separation of 100 m. The data contain shallow 3D high-velocity channels at a depth of around 1500 m. These

channels produce pull-up on what appear to be otherwise smooth sub-horizontal reflectors beneath, and on the deeper reservoir (not shown). The channels also produce a characteristic w-pattern in high resolution stacking velocity analysis, figure 2. The combined effect of the pull up and distorted velocity analysis compromises imaging of the reservoir, and has prevented accurate depth migration leading to increased uncertainty in reserve estimation. The velocity structure within the channels appears laterally complicated, and it has not been satisfactorily resolved using reflection tomography or migration velocity analysis.

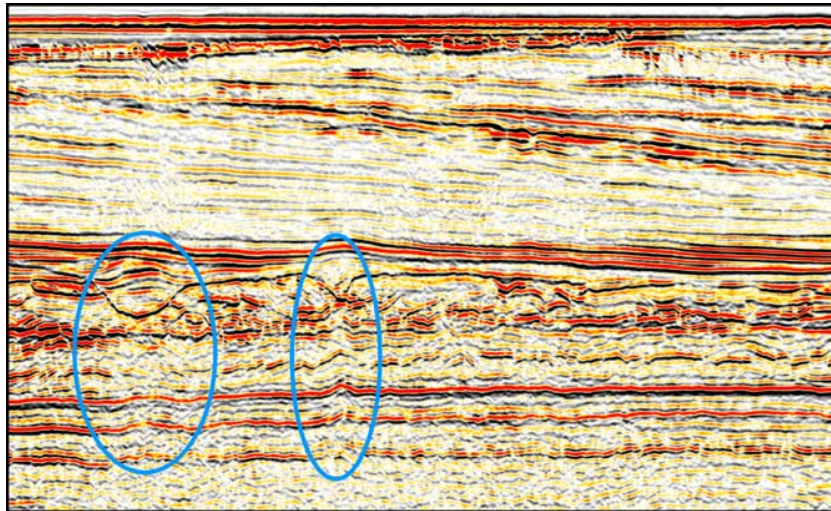


**Figure 1** A 2D slice through a 3D seismic survey showing shallow high-velocity channels that produce clear velocity distortion in the pre-stack time migrated image of deeper sub-horizontal reflectors.

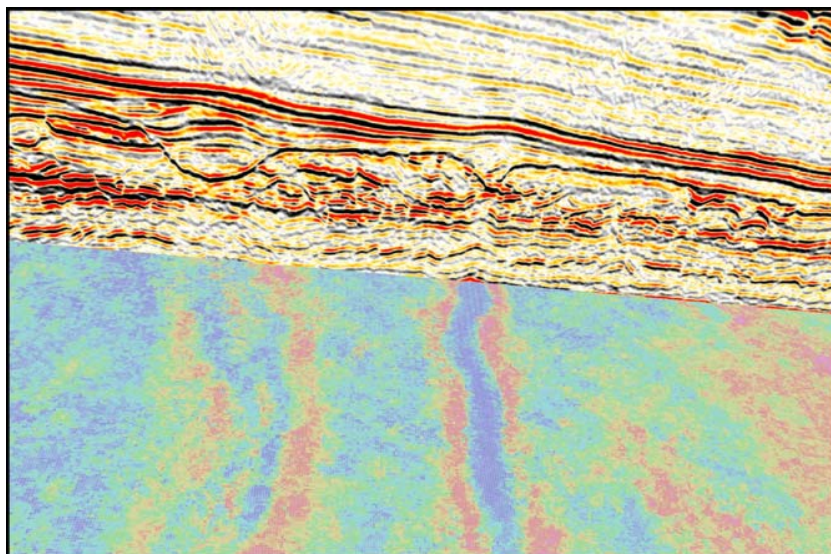


**Figure 2** High-resolution stacking-velocity analysis at 2000 ms beneath the shallow channels. The velocity structure in the channels produces a characteristic spurious w-structure in the deeper velocities.

Full-wavefield tomography has been applied to this dataset, and the results of applying the resulting velocity model are shown in figure 3.

The left panel shows the results of depth converting the data using results from conventional velocity analysis. There is clear but complicated velocity distortion of the event at the base of this section underneath the channel.

The right panel shows the same data depth converted using the high-resolution velocity model obtained from wavefield inversion. Using this velocity model, the reflector at 2200 m appears much simpler in depth, and the velocity distortion produced by the channel appears to have disappeared.

Within the channel itself, the reflector geometry is also subtly but significantly different. In the right figure, the channel appears to show the effects of clear and systematic differential compaction which is not easily evident in figure on the left, and the structure of the double sub-channel within the main channel is both clearer and more geologically plausible.

We conclude that the waveform tomography is producing a high-resolution velocity model that more faithfully represents the sub-surface. We have not yet depth migrated the reservoir section with the wavefield tomographic model, but expect to obtain a higher fidelity image when we do.

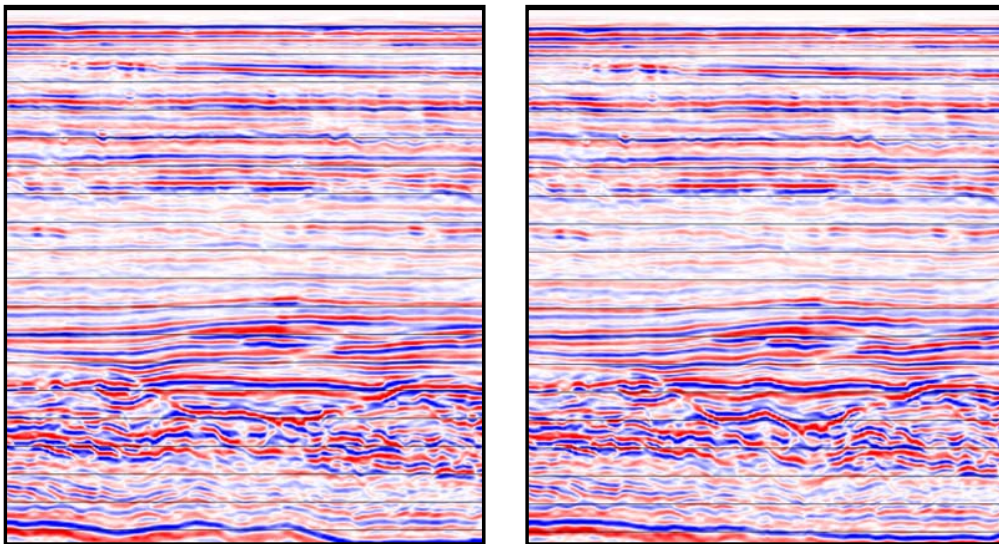


**Figure 3** A close up of the pre-stack, time-migrated image of one of the channels and underlying sub-horizontal reflector. The panel on the left has been depth converted using the original conventionally obtained velocity model. The panel on the right has been depth converted using the high-resolution velocity model obtained from wavefield tomography – the spurious structure on the underlying reflectors has disappeared, and the geological structure within the channel itself appears more reasonable.